Journal of the Brazilian Society of Mechanical Sciences and Engineering (2018) 40:296
https://doi.org/10.1007/s40430-018-1222-5

TECHNICAL PAPER

Effect of thickness stretching on the static deformations, natural frequencies, and critical buckling loads of laminated composite and sandwich beams

Atteshamuddin Shamshuddin Sayyad[1] · Yuwaraj Marotrao Ghugal[2]

Received: 8 November 2016 / Accepted: 22 March 2018 / Published online: 15 May 2018

Abstract

The present study investigates the bending, buckling, and vibration responses of shear deformable laminated composite and sandwich beams using trigonometric shear and normal deformation theory. The most important feature of the present theory is that it includes the effects of transverse shear and normal deformations, i.e., the effect of thickness stretching. Therefore, the theory is also called as a quasi-2D theory. The axial displacement uses sine function in terms of the thickness coordinate to include the effect of transverse shear deformation, and the transverse displacement uses cosine function in terms of the thickness coordinate to include the effect of transverse normal deformation, i.e., the thickness stretching. The present theory satisfies the zero shear stress conditions at top and bottom surfaces of the beam without using shear correction factor. Governing differential equations and associated boundary conditions of the theory are derived by employing the dynamic version of principle of virtual work. Navier-type closed-form solutions are obtained for simply supported boundary conditions. The numerical results are obtained for deflections, stresses, natural frequencies, and critical buckling loads for isotropic, laminated composite, and sandwich beams. Since exact elasticity solutions for laminated composite and sandwich beams are not available in the literature, the results are compared with those obtained by using other higher-order shear deformation theories to demonstrate the accuracy of the proposed theory.

Keywords Thickness stretching · Laminated · Sandwich · Bending · Buckling · Vibration

1 Introduction

Laminated composite and sandwich beams are being widely used in many industries due to their attractive properties such as high strength and stiffness-to-weight ratio. The effects of transverse shear deformation and thickness stretching are more pronounced in the thick beams. Therefore, static bending, free vibration, and buckling analysis of laminated composite and sandwich thick beams have received widespread attention in recent years. Analysis of composite beams is difficult by using three-dimensional (3D) elasticity theory due to complex mathematics. Therefore, still 3D elasticity solutions for the bending, buckling, and free vibration analysis of laminated composite and sandwich beams are not available in the literature. This led to the development of approximate beam theories for the analysis of beams. Various beam theories are developed by the researchers for the analysis of laminated composite and sandwich beams. Recently, these theories are reviewed by Sayyad and Ghugal [1].

The effects of shear deformation and thickness stretching are neglected by classical thin beam theory (CBT) developed by Bernoulli–Euler [2, 3]. Timoshenko [4, 5] was the first person who considered the effect of shear deformation in his first order shear deformation theory (FSDT) which is also called as Timoshenko beam theory (TBT). But this theory needs shear correction factor and gives constant shear strain through the thickness. These limitations of CBT and TBT led the foundation for the

Technical Editor: André Cavalieri.

✉ Atteshamuddin Shamshuddin Sayyad
attu_sayyad@yahoo.co.in

1 Department of Civil Engineering, SRES's Sanjivani College of Engineering, Savitribai Phule Pune University, Kopargaon, Maharashtra 423601, India

2 Department of Applied Mechanics, Government College of Engineering, Shivaji University, Kolhapur, Karad, Maharashtra 415124, India

development of refined beam theories. Several higher-order shear deformation theories (HSDTs) are developed by researchers which consider the effect of transverse shear deformation. These HSDTs are classified as equivalent single-layer theories, layerwise theories, and zigzag theories. The present study deals with the analysis of composite beams using equivalent single-layer theories.

1.1 Motivation of the present study

It can be noted that an initiation of delamination in multilayered composite structures is caused due to interlaminar transverse shear and normal stresses. Therefore, any refinement of classical models is meaningless, in general, unless the effects of interlaminar continuous transverse shear and normal stresses are both taken into account in a multilayered beam theory [6–8]. However, no consideration is given to the effect of transverse normal deformation/strain ($\varepsilon_z \neq 0$) in higher-order beam theories existing in the literature when these theories are applied to laminated composite and sandwich beams in view of minimizing the number of unknown variables. Therefore, refined theories which consider the effects of transverse normal deformations, i.e., thickness stretching, need more attention. Table 1 shows the review of various beam theories available in the literature.

1.2 Novelty of the present theory and major contributions

1. From Table 1, it is pointed out that very few theories are available in the literature which consider the effects of transverse normal deformation. Also, most of them are applied for the analysis of plates. It can be noted that the well-known theory of Reddy [11] also neglects the effect of transverse normal deformation. Therefore, the present study focuses on the study of the effects of transverse shear and normal deformations on static deformation, natural frequencies, and critical buckling loads of laminated composite and sandwich beams using trigonometric shear and normal deformation theory.
2. The most important feature of the present theory is that it includes the effects of transverse shear and normal deformations, i.e., the effect of thickness stretching. The axial displacement uses sine function in terms of the thickness coordinate to include the effect of transverse shear deformation, and the transverse displacement uses cosine function in terms of the thickness coordinate to include the effect of transverse normal deformation, i.e., thickness stretching.
3. The kinematics of the present theory is much richer than those of the other higher-order shear deformation theories, because if the trigonometric term is expanded in power series, the kinematics of higher-order theories is implicitly taken into account to good deal of extent.
4. In polynomial-type higher-order shear deformation theories, it needs to be noted that not only every additional power of thickness coordinate in the displacement field introduces an additional unknown variable in those theories, but these variables are also difficult to interpret physically. Thus, the use of the sinusoidal function (non-polynomial type) in terms of thickness coordinate enhances the richness of the theory and also results in reduction in the number of unknown variables as compared to other type of displacement-based higher-order theories without loss of physics of the problem in modeling.
5. The present theory satisfies the zero shear stress conditions at top and bottom surfaces of the beam without using problem-dependent shear correction factor.
6. The estimation of through-the-thickness distributions of interlaminar transverse shear and normal stresses using equations of equilibrium of the theory of elasticity has not been studied satisfactorily by the

Table 1 Review of various beam theories with and without normal deformation effect (ε_z)

References	Effect of thickness stretching (ε_z)	Effect of shear deformation (γ_{xz})
Bernoulli [2] and Euler [3]	Not considered ($\varepsilon_z = 0$)	Not considered ($\gamma_{xz} = 0$)
Timoshenko [4, 5], Levinson [9], Krishna Murty [10], Reddy [11], Kant and Manjunatha [12], Ghugal and Shimpi [13], Sayyad and Ghugal [14], Soldatos and Elishakoff [15], Karama et al. [16], Sayyad and Ghugal [17], Sayyad [18], Benatta et al. [19, 20], Aydogdu [21], Mahi et al. [22], Shi and Voyiadjis [23], Sayyad et al. [24–26], Vo and Thai [27], Akavci [28], Ray [29], Mantari et al. [30–32], Meiche et al. [33], Daouadji et al. [34], Thai et al. [35], etc.	Not considered ($\varepsilon_z = 0$)	Considered ($\gamma_{xz} \neq 0$)
Carrera [6–8], Kant and Manjunatha [36], Zenkour [37, 38], Maiti and Sinha [39], Sayyad and Ghugal [40], Vo et al. [41], Neves et al. [42, 43], etc.	Considered ($\varepsilon_z \neq 0$)	Considered ($\gamma_{xz} \neq 0$)

various researchers as can be seen from the open literature. Evaluation of these interlaminar stresses in the present study is an important contribution.

7. The study of global response of softcore sandwich structures is a challenging problem in physical modeling, especially using simplified (1D or 2D) theories, rather than 3D elasticity. In the present study, deflections, interlaminar stresses, natural frequencies of various modes of vibration and critical buckling loads are obtained for softcore sandwich beams which can be served as benchmark solutions and can be treated as another important contribution of the present study.

In the present study, governing differential equations and associated boundary conditions of the theory are derived by employing the dynamic version of principle of virtual work and the fundamental lemma of calculus of variations. Navier-type closed-form solutions are obtained for simply supported isotropic, laminated composite, and sandwich beams. The results of displacements, stresses, natural frequencies, and critical buckling loads are compared with the theories existing in literature [44–58] to demonstrate the accuracy of the proposed theory.

2 Beam under consideration

Consider a beam of rectangular cross section ($b \times h$) and span L as shown in Fig. 1. The beam is composed of N number of thin layers perfectly bonded together. The beam is assumed in a Cartesian coordinate system where the x-, y-, and z-axes are taken along the length, the width, and the thickness of the beam, respectively. The z-axis is taken downward positive. The beam is subjected to transverse loading $q\ (x)$ on the upper surface of the beam in case of bending and subjected to axial compressive forces (N_x^0) in case of buckling. The transverse and axial loads are assumed to be zero for the free vibration analysis.

2.1 Kinematics of the present beam theory

The displacement field of the present trigonometric shear and normal deformation theory is given as:

$$u(x,z,t) = u_0(x,t) + u_b(x,z,t) + u_s(x,z,t)$$
$$w(x,z,t) = w_0(x,t) + w_s(x,z,t) \quad (1)$$

where u_0 is the axial displacement of the neutral axis along x-axis, u_b is the bending component analogous to the Euler–Bernoulli beam theory, and u_s is the shear component assumed to be sinusoidal in nature with respect to thickness coordinate. The transverse displacement w in z direction is assumed to be a function of x and z coordinates. Therefore, the displacement field of the present trigonometric shear and normal deformation beam theory takes the following form.

$$u(x,z,t) = u_0 - z w_{0,x} + f(\bar{z})\,\phi(x,t),$$
$$w(x,z,t) = w_0(x,t) + g(\bar{z})\,\xi(x,t) \quad (2)$$

where u_0, w_0, ϕ and ξ are the four unknown displacement functions of the neutral axis of the beam, while $f(\bar{z})$ and $g(\bar{z})$ represent functions determining the distribution of the

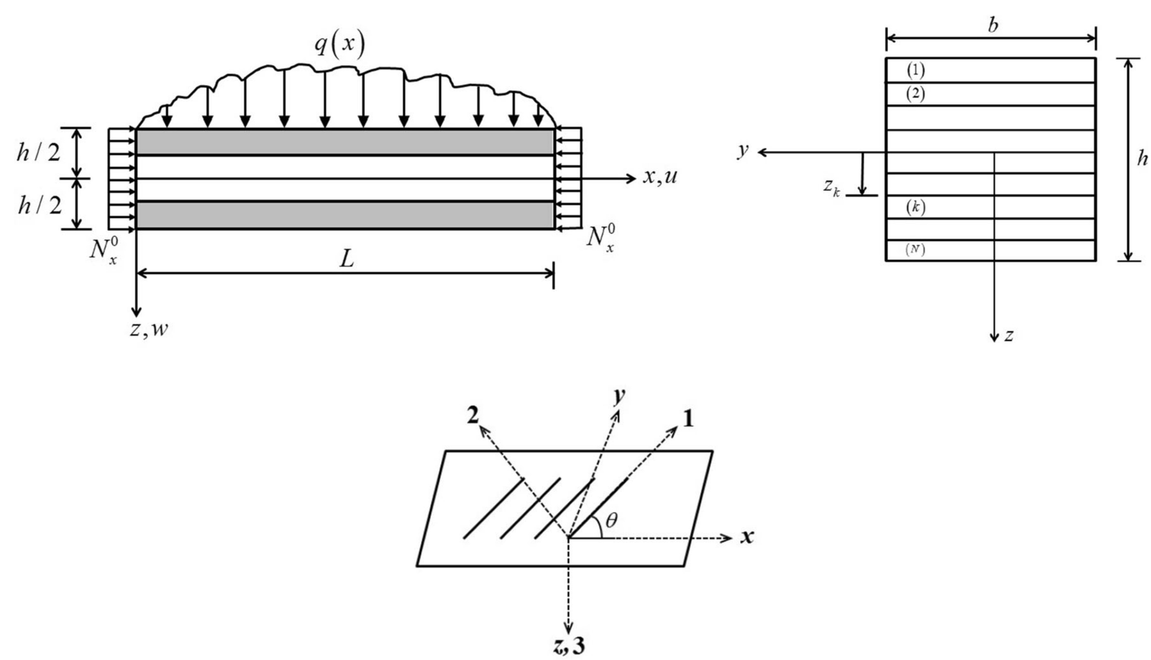

Fig. 1 Beam geometry, lamina material axes, and laminate reference axes

transverse shear and normal stresses along the thickness of the beam. When transverse displacement w is a function of z coordinate, transverse normal strain ε_z is not equal to zero which represent the thickness stretching effect. The kinematics proposed in Eq. (2) is strongly based on solution of three-dimensional Navier's equations of elastostatics for thick plate under flexure presented by Cheng [59] which involves transverse shear stress and transverse normal stress. The kinematics of proposed theory is the reduction problem from three-dimensional considerations to one-dimensional one. Hence, the theory represented by Eq. (2) is correct deduction from the three- dimensional elasticity for thick plate.

The nonzero strain components associated with the present displacement field are as follows:

$$\begin{aligned} \varepsilon_x &= \varepsilon_x^0 + z\varepsilon_x^1 + f(\bar{z})\,\varepsilon_x^2, \\ \varepsilon_z &= g'(\bar{z})\,\xi, \\ \gamma_{xz} &= g(\bar{z})\gamma_{xz}^0 + f'(\bar{z})\phi \end{aligned} \tag{3}$$

where

$$\begin{aligned} &\varepsilon_x^0 = u_{0,x}, \quad \varepsilon_x^1 = -w_{0,xx}, \quad \varepsilon_x^2 = \phi_{,x}, \quad \gamma_{xz}^0 = \xi_{,x}, \\ &f(\bar{z}) = (h/\pi)\sin(\pi\bar{z}) \quad \text{and} \quad g(\bar{z}) = (h/\pi)\cos(\pi\bar{z}) \end{aligned} \tag{4}$$

where $\bar{z} = z/h$ and '$_{,x}$' represents the derivative with respect to x. Here, $\varepsilon_z \neq 0$ shows that the present theory considered the effect of transverse normal deformation, i.e., thickness stretching. Many well-known theories neglect this effect as shown in Table 1.

2.2 Constitutive relations

Since the present theory considered the effects of both transverse shear and normal deformations, a two-dimensional Hooke's law is used to obtained stress quantities in the beam domain. The laminate is made of several orthotropic layers. The constitutive relations in the kth layer of laminate are given as:

$$\begin{Bmatrix} \sigma_x \\ \sigma_z \\ \tau_{xz} \end{Bmatrix}^{(k)} = \begin{bmatrix} Q_{11} & Q_{13} & 0 \\ Q_{13} & Q_{33} & 0 \\ 0 & 0 & Q_{55} \end{bmatrix}^{(k)} \begin{Bmatrix} \varepsilon_x \\ \varepsilon_z \\ \gamma_{xz} \end{Bmatrix}^{(k)} \tag{5}$$

where $\{\sigma\}^{(k)}$ is the stress vector, $\{\varepsilon\}^{(k)}$ is the strain vector and $[Q_{ij}]^{(k)}$ is the transformed rigidity matrix. The elements of transformed rigidity matrix are as follows:

$$\begin{aligned} &Q_{11} = \frac{E_1}{1-\mu_{13}\,\mu_{31}}; \quad Q_{13} = \frac{\mu_{13}E_3}{1-\mu_{13}\,\mu_{31}}; \\ &Q_{33} = \frac{E_3}{1-\mu_{13}\,\mu_{31}}; \quad Q_{55} = G_{13} \end{aligned} \tag{6}$$

Here $E_i, G_{ij}, \mu_{ij}\ (i,j = 1,3)$ are the material properties of lamina and 1, 2, 3 are the lamina fiber (material) axes, and x, y, z are the laminate reference axes (see Fig. 1). The principal material axes of lamina (1, 2, 3) may not coincide with the reference axes of the laminate (x, y, z) in case of angle ply laminates. It is therefore necessary to transform the constitutive relations from lamina fiber axes to laminate reference axes.

2.3 Equations of motion

The equations of motion of the proposed theory are derived using dynamic version of principle of virtual work. The principle of virtual work is applied in the following analytical form:

$$\begin{aligned} &\sum_{k=1}^{N} b \int_{h_k}^{h_{k+1}} \int_0^L \left[\sigma_x^k \delta\varepsilon_x + \sigma_z^k \delta\varepsilon_z + \tau_{xz}^k \delta\gamma_{zx}\right] \mathrm{d}x\mathrm{d}z \\ &\quad - \int_0^L q(x)\delta w \mathrm{d}x + \rho^{(k)} \sum_{k=1}^{N} \int_{h_k}^{h_{k+1}} \int_0^L \left[u_{,tt}\delta u + w_{,tt}\delta w\right] \mathrm{d}x\mathrm{d}z \\ &\quad - \int_0^L N_x^0 w_{,x} \delta w_{0,x} \mathrm{d}x = 0 \end{aligned} \tag{7}$$

where ρ is the mass per unit volume and δ denotes the variational operator. Substituting expressions for virtual strains and displacements into the Eq. (7) and introducing stress resultants, one can write:

$$\begin{aligned} &\int_0^L \left[N_x \delta u_{0,x} - M_x^{c} \delta w_{0,xx} + M_x^{s} \delta\phi_{,x} + V_z \delta\xi + V_x \delta\xi_{,x} \right. \\ &\left. + V_x \delta\phi\right] \mathrm{d}x \\ &\quad - \int_0^L q(x)\delta w \mathrm{d}x + I_1 \int_0^L \left(u_{0,tt}\delta u_0 + w_{0,tt}\delta w_0\right) \mathrm{d}x \\ &\quad - I_2 \int_0^L \left(u_{0,tt}\delta w_{0,x} + w_{0,xtt}\delta u_0\right) \mathrm{d}x \\ &\quad + I_3 \int_0^L \left(u_{0,tt}\delta\phi + \phi_{,tt}\delta u_0\right) \mathrm{d}x + I_4 \int_0^L w_{0,xtt}\delta w_{0,x} \mathrm{d}x \\ &\quad - I_5 \int_0^L \left(w_{0,xtt}\delta\phi + \phi_{,tt}\delta w_{0,x}\right) \mathrm{d}x \\ &\quad + I_6 \int_0^L \left(w_{0,tt}\delta\xi + \xi_{,tt}\delta w_0\right) \mathrm{d}x \\ &\quad + I_7 \int_0^L \phi_{,tt}\delta\phi \mathrm{d}x + I_8 \int_0^L \xi_{,tt}\delta\xi \mathrm{d}x - N_x^0 \int_0^L w_{,x}\delta w_{0,x} \mathrm{d}x \\ &\quad = 0 \end{aligned} \tag{8}$$

Integrating the Eq. (8) by parts and setting the coefficients of δu_0, δw_0, $\delta\phi$ and $\delta\xi$ equal to zero, the following governing equations and boundary conditions are obtained:

$$\begin{aligned}
&\delta u_0 : \mathrm{N}_{x,x} = I_1 u_{0,tt} - I_2 w_{0,xtt} + I_3 \phi_{,tt} \\
&\delta w : \mathrm{M}^{c}_{x,xx} + \mathrm{q} - N^0_x w_{0,xx} = I_2 u_{0,xtt} - I_4 w_{0,xxtt} \\
&\quad + I_1 w_{0,tt} + I_5 \phi_{,xtt} + I_6 \xi_{,tt} \\
&\delta \phi : \mathrm{M}^{s}_{x,x} - \mathrm{V}_x = I_3 u_{0,tt} - I_5 w_{0,xtt} + I_7 \phi_{,tt} \\
&\delta \xi : \mathrm{V}_{x,x} - \frac{\pi}{h} V_z = I_6 w_{0,tt} + I_8 \xi_{,tt}
\end{aligned} \tag{9}$$

where N_x is the axial force resultant, M^c_x is the moment resultant analogous to classical beam theory; M^s_x is the refined moment due to transverse shear deformation effect, V_x and V_z are the shear force resultants due to transverse shear deformation and transverse normal deformation effects, respectively. These force and moment resultants acting on the cross section of the laminate are defined as:

$$\begin{aligned}
N_x &= \sum_{k=1}^{N} \int_{h_k}^{h_{k+1}} \sigma^k_x \mathrm{d}z = A_{11} u_{0,x} - B_{11} w_{0,xx} + As_{11} \phi_{,x} - \frac{\pi}{h} As_{12} \xi \\
M^c_x &= \sum_{k=1}^{N} \int_{h_k}^{h_{k+1}} \sigma^k_x z \mathrm{d}z = B_{11} u_{0,x} - D_{11} w_{0,xx} + Bs_{11} \phi_{,x} - \frac{\pi}{h} Bs_{12} \xi \\
M^s_x &= \sum_{k=1}^{N} \int_{h_k}^{h_{k+1}} \sigma^k_x f(\bar{z}) \mathrm{d}z = As_{11} u_{0,x} - Bs_{11} w_{0,xx} + Ass_{11} \phi_{,x} - \frac{\pi}{h} Ass_{12} \xi \\
V_x &= \sum_{k=1}^{N} \int_{h_k}^{h_{k+1}} \tau^k_{xz} f'(\bar{z})\,\mathrm{d}z = Acc_{55} \left(\phi + \frac{h}{\pi} \xi_{,x} \right) \\
V_z &= \sum_{k=1}^{N} \int_{h_k}^{h_{k+1}} \sigma^k_{zz} g'(\bar{z})\,\mathrm{d}z = -\frac{\pi}{h} \left[As_{12} u_{0,x} - Bs_{12} w_{0,xx} + Ass_{12} \phi_{,x} - \frac{\pi}{h} Ass_{22} \xi \right] \\
Q_x &= M^c_{x,x} = B_{11} u_{0,xx} - D_{11} w_{0,xxx} + Bs_{11} \phi_{,xx} - \frac{\pi}{h} Bs_{12} \xi_{,x}
\end{aligned} \tag{10}$$

The boundary conditions at the supports ($x = 0$ and $x = L$) of the beam are of the following form:

Either $N_x = 0$ or $u_0 = 0$ is prescribed (11)

Either $V_x = 0$ or $w = 0$ is prescribed (12)

Either $M^c_x = 0$ or $w_{,x} = 0$ is prescribed (13)

Either $M^s_x = 0$ or $\phi = 0$ is prescribed (14)

Either $V_z = 0$ or $\xi = 0$ is prescribed (15)

The governing equations in terms of unknown variables (u_0, w_0, ϕ and ξ) are obtained as follows:

$$\begin{aligned}
&-A_{11} u_{0,xx} + B_{11} w_{0,xxx} - As_{11} \phi_{,xx} + As_{13} \frac{\pi}{h} \xi_{,x} + I_1 u_{0,tt} \\
&\quad - I_2 w_{0,xtt} + I_3 \phi_{,tt} \\
&\quad = 0
\end{aligned} \tag{16}$$

$$\begin{aligned}
&-B_{11} u_{0,xxx} + D_{11} w_{0,xxxx} - Bs_{11} \phi_{,xxx} + \frac{\pi}{h} Bs_{13} \xi_{,xx} + I_2 u_{0,xtt} \\
&\quad - I_4 w_{0,xxtt} + I_1 w_{0,tt} + I_5 \phi_{,xtt} \\
&\quad = q + N^0_x w_{0,xx}
\end{aligned} \tag{17}$$

$$\begin{aligned}
&-As_{11} u_{0,xx} + Bs_{11} w_{0,xxx} - Ass_{11} \phi_{,xx} + Acc_{55} \phi + Ass_{13} \frac{\pi}{h} \xi_{,x} \\
&\quad + Acc_{55} \frac{h}{\pi} \xi_{,x} + I_3 u_{0,tt} - I_5 w_{0,xtt} + I_7 \phi_{,tt} \\
&\quad = 0
\end{aligned} \tag{18}$$

$$\begin{aligned}
&-\frac{\pi}{h} As_{13} u_{0,x} + \frac{\pi}{h} Bs_{13} w_{0,xx} - \left(\frac{\pi}{h} Ass_{13} + \frac{h}{\pi} Acc_{55} \right) \phi_{,x} \\
&\quad - \frac{h^2}{\pi^2} Acc_{55} \xi_{,xx} + \frac{\pi^2}{h^2} Ass_{33} \xi + I_6 w_{0,tt} + I_8 \xi_{,tt} \\
&\quad = 0
\end{aligned} \tag{19}$$

where the beam stiffness and inertia constants are defined as follows:

$$\begin{aligned}
&\{ A_{ij} \quad B_{ij} \quad D_{ij} \} = \sum_{k=1}^{N} \int_{h_k}^{h_{k+1}} Q^{(k)}_{ij} \{ 1 \quad z \quad z^2 \} \mathrm{d}z, \quad (i,j = 1,3), \\
&\{ As_{ij} \quad Bs_{ij} \} = \sum_{k=1}^{N} \int_{h_k}^{h_{k+1}} Q^{(k)}_{ij} f(\bar{z}) \{ 1 \quad z \} \mathrm{d}z, \quad (i,j = 1,3), \\
&\{ Ass_{ij} \} = \sum_{k=1}^{N} \int_{h_k}^{h_{k+1}} Q^{(k)}_{ij} f^2(\bar{z}) \mathrm{d}z, \quad (i,j = 1,3), \\
&\{ Acc_{ij} \} = \sum_{k=1}^{N} \int_{h_k}^{h_{k+1}} Q^{(k)}_{ij} [f'(\bar{z})]^2 \mathrm{d}z \quad (i,j = 5)
\end{aligned} \tag{20}$$

$$\begin{aligned}
&I_1 = \sum_{k=1}^{N} \rho^{(k)} \int_{h_k}^{h_{k+1}} \mathrm{d}z, \quad I_2 = \sum_{k=1}^{N} \rho^{(k)} \int_{h_k}^{h_{k+1}} z \mathrm{d}z, \\
&\quad I_3 = \sum_{k=1}^{N} \rho^{(k)} \int_{h_k}^{h_{k+1}} f(\bar{z}) \mathrm{d}z, \\
&I_4 = \sum_{k=1}^{N} \rho^{(k)} \int_{h_k}^{h_{k+1}} z^2 \mathrm{d}z, \quad I_5 = \sum_{k=1}^{N} \rho^{(k)} \int_{h_k}^{h_{k+1}} z f(\bar{z}) \mathrm{d}z, \\
&\quad I_6 = \sum_{k=1}^{N} \rho^{(k)} \int_{h_k}^{h_{k+1}} g(\bar{z}) \mathrm{d}z, \\
&I_7 = \sum_{k=1}^{N} \rho^{(k)} \int_{h_k}^{h_{k+1}} f^2(\bar{z}) \mathrm{d}z, \quad I_8 = \sum_{k=1}^{N} \rho^{(k)} \int_{h_k}^{h_{k+1}} g^2(\bar{z}) \mathrm{d}z.
\end{aligned} \tag{21}$$

2.4 Closed-form solution

The solution which satisfies governing differential equations at any point of the beam can be either in the form of a finite or infinite series. The solutions expressed in terms of finite number of terms are called as closed-form solutions. In the present study, Navier's solution technique is employed to obtain the closed-form solution. Navier's solution for the simply supported laminated composite and sandwich beam is developed satisfying the following boundary conditions.

$$\text{at } x = 0 \text{ and } x = L: \; N_x = w_0 = \xi = M_x^{c} = M_x^{s} = 0 \tag{22}$$

The transverse distributed load is expanded using the Fourier sine series as

$$q(x) = \sum_{m=1,3,5}^{\infty} \begin{cases} q_0 \sin\alpha x & (m=1) & \text{for sinusoidal loading} \\ \dfrac{4q_0}{m\pi}\sin\alpha x & (m = 1,3,5\ldots) & \text{for uniform loading} \end{cases} \tag{23}$$

where q_0 is the maximum intensity of the distributed load. Following the Navier's solution procedure, the trigonometric forms of displacement variables u_0, w_0, ϕ and ξ that satisfy the boundary conditions exactly are given by:

$$u_0(x,t) = \sum_{m=1}^{\infty} u_m \cos\alpha x e^{i\omega t}, \quad w(x,t) = \sum_{m=1}^{\infty} w_m \sin\alpha x e^{i\omega t},$$
$$\phi(x,t) = \sum_{m=1}^{\infty} \phi_m \cos\alpha x e^{i\omega t}, \quad \xi(x,t) = \sum_{m=1}^{\infty} \xi_m \sin\alpha x e^{i\omega t} \tag{24}$$

where $\alpha = m\pi/L$, $i = \sqrt{-1}$, ω is the natural frequency and u_m, w_m, ϕ_m and ξ_m are the unknown coefficients to be determined. The time-dependent part of Eq. (24) is used only for the free vibration problem; otherwise, it is omitted. The transverse load $q(x)$ is used only for bending analysis, otherwise discarded for the vibration and buckling analysis. For the buckling analysis of beam, both transverse load and time-dependent terms are omitted. Substituting this form of solution into the governing Eqs. (16)–(19) yields a set of algebraic equations which can be written in matrix form as follows:

Bending analysis of beam:

$$[K]\{\Delta\} = \{f\} \; (\text{by setting } N_x^0 \text{ and } \omega \text{ equal to zero}) \tag{25}$$

Free vibration analysis of beam:

$$\left([K] - \omega^2[M]\right)\{\Delta\} = \{0\} \quad (\text{by setting } N_x^0 \text{ and } q(x) \text{ equal to zero}) \tag{26}$$

Buckling analysis of beam:

$$([K] - N_0[N])\{\Delta\} = \{0\} \; (\text{by setting } \omega = q(x) = 0 \text{ and } N_x^0 = N_0) \tag{27}$$

where $[K]$ is the stiffness matrix, $\{f\}$ is the force vector, $[M]$ is the mass matrix, $[N]$ is the geometric matrix due to the axial forces, ω is the natural frequency and N_0 is the buckling load factor. These matrices are defined as follows:

$$[K] = \begin{bmatrix} A_{11}\alpha^2 & -B_{11}\alpha^3 & As_{11}\alpha^2 & \frac{\pi}{h}As_{13}\alpha \\ -B_{11}\alpha^3 & D_{11}\alpha^4 & -Bs_{11}\alpha^3 & -\frac{\pi}{h}Bs_{13}\alpha^2 \\ As_{11}\alpha^2 & -Bs_{11}\alpha^3 & (Ass_{11}\alpha^2 + Acc_{55}) & \left(\frac{\pi}{h}Ass_{13} + \frac{h}{\pi}Acc_{55}\right)\alpha \\ \frac{\pi}{h}As_{13}\alpha & -\frac{\pi}{h}Bs_{13}\alpha^2 & \left(\frac{\pi}{h}Ass_{13} + \frac{h}{\pi}Acc_{55}\right)\alpha & \left(\frac{h^2}{\pi^2}Acc_{55}\alpha^2 + \frac{\pi^2}{h^2}Ass_{33}\right) \end{bmatrix} \tag{28}$$

$$\{\Delta\} = \begin{Bmatrix} u_m \\ w_m \\ \phi_m \\ \xi_m \end{Bmatrix} \tag{29}$$

$$\{f\} = \begin{Bmatrix} 0 \\ q_m \\ 0 \\ 0 \end{Bmatrix} \tag{30}$$

$$[M] = \begin{bmatrix} I_1 & -I_2\frac{m\pi}{L} & I_3 & 0 \\ -I_2\frac{m\pi}{L} & \left(I_4\frac{m^2\pi^2}{L^2} + \mathrm{I}_1\right) & -I_5\frac{m\pi}{L} & I_6 \\ I_3 & -I_5\frac{m\pi}{L} & I_7 & 0 \\ 0 & I_6 & 0 & I_8 \end{bmatrix} \tag{31}$$

$$[N] = \begin{bmatrix} 0 & 0 & 0 & 0 \\ 0 & \alpha^2 & 0 & 0 \\ 0 & 0 & 0 & 0 \\ 0 & 0 & 0 & 0 \end{bmatrix} \tag{32}$$

3 Numerical results and discussion

In this section, the efficiency of the present theory is proved in predicting the displacements, stresses, natural frequencies, and critical buckling loads of simply supported laminated composite and sandwich beams. The numerical results obtained by using the present theory are compared with those existing in literature. The material properties shown in Table 2 are used in the various illustrated examples. Numerical investigations have been undertaken on bending, free vibration, and buckling analysis of isotropic, laminated composite, and sandwich beams with different material properties and different lamination schemes, namely:

Problem 1: Bending of isotropic beam
Problem 2: Bending of laminated composite beams.
Problem 3: Bending of sandwich beams.
Problem 4: Free vibration of laminated composite beams.
Problem 5: Free vibration of sandwich beams.
Problem 6: Buckling of laminated composite and sandwich beams.

Table 2 Material properties of isotropic, laminated composite, and sandwich beams

Material	References	Elastic properties
1	[11, 13]	$E_1 = E_2 = E_3 = 210$ GPa, $G_{12} = G_{13} = G_{23} = 80.769$ GPa, $\mu_{12} = \mu_{13} = \mu_{23} = 0.3$
2	[44]	$E_1 = 172.4$ GPa, $E_2 = E_3 = 6.89$ GPa, $G_{12} = G_{13} = 3.45$ GPa, $G_{23} = 1.378$ GPa, $\mu_{12} = \mu_{13} = \mu_{23} = 0.25$, ρ = constant
3	[44]	$E_1 = E_2 = 0.276$ GPa, $E_3 = 3.45$ GPa, $G_{12} = 0.1104$ GPa, $G_{13} = G_{23} = 0.414$ GPa, $\mu_{12} = \mu_{13} = \mu_{23} = 0.25$, ρ = constant
4	[47]	E_1/E_2 = Open, $E_3 = E_2$, $G_{12} = G_{13} = 0.6\ E_2$, $G_{23} = 0.5\ E_2$, $\mu_{12} = \mu_{13} = \mu_{23} = 0.25$, ρ = constant
5	[53, 54]	$E_1 = 144.80$ GPa, $E_2 = E_3 = 9.65$ GPa, $G_{12} = G_{13} = 4.14$ GPa, $G_{23} = 3.45$ GPa, $\mu_{12} = \mu_{13} = \mu_{23} = 0.3$, $\rho = 1389.23$ kg/m^3
6	[56]	$E_1 = 131$ GPa, $E_2 = E_3 = 10.34$ GPa, $G_{12} = G_{23} = 6.895$ GPa, $G_{23} = 6.205$ GPa, $\mu_{12} = \mu_{13} = 0.22$, $\mu_{23} = 0.49$, $\rho = 1000$ kg/m^3
7	[56]	$E_1 = 0.2208$ MPa, $E_2 = 0.2001$ MPa, $E_3 = 2760$ MPa, $G_{12} = 16.56$ MPa, $G_{13} = 545.1$ MPa, $G_{23} = 455.4$ MPa, $\mu_{12} = 0.99$, $\mu_{13} = \mu_{23} = 0.00003$, $\rho = 70$ kg/m^3

Table 3 Comparison of axial displacement, transverse displacement, axial stress, and transverse shear stress for isotropic beam of rectangular cross section

L/h	Source	Sinusoidal loading				Uniform loading			
		$\bar{u}^{max}$	$\bar{w}^{max}$	$\bar{\sigma}_x^{max}$	$\bar{\tau}_{xz}^{max}$	$\bar{u}^{max}$	$\bar{w}^{max}$	$\bar{\sigma}_x^{max}$	$\bar{\tau}_{xz}^{max}$
4	Present ($\varepsilon_z \neq 0$)	12.456	1.409	10.135	1.889	16.159	1.782	12.445	2.635
	Reddy [11]	12.715	1.429	9.9860	1.897	16.504	1.806	12.263	2.795
	Ghugal and Shimpi [13]	12.736	1.429	10.003	1.895	16.540	1.806	12.276	3.778
	Kant et al. [44]	–	1.410	9.907	1.900	–	1.783	12.200	2.814
	Timoshenko [4]	12.385	1.430	9.727	1.910	16.000	1.806	12.000	2.953
	Bernoulli–Euler [2, 3]	12.385	1.232	9.727	1.910	16.000	1.563	12.000	2.953
10	Present ($\varepsilon_z \neq 0$)	193.437	1.259	62.077	4.748	249.990	1.596	76.544	7.216
	Reddy [11]	194.337	1.264	61.053	4.770	251.270	1.602	75.268	7.304
	Ghugal and Shimpi [13]	194.389	1.263	61.069	4.769	251.370	1.601	75.276	7.326
	Kant et al. [44]	–	1.261	60.990	4.771	–	1.598	75.250	7.244
	Timoshenko [4]	193.510	1.264	60.793	4.775	250.000	1.602	75.000	7.383
	Bernoulli–Euler [2, 3]	193.509	1.232	60.793	4.775	250.000	1.563	75.000	7.383
20	Present ($\varepsilon_z \neq 0$)	1546.26	1.237	247.606	9.503	1997.77	1.569	305.43	14.648
	Kant et al. [44]	–	1.239	243.360	9.548	–	1.571	300.24	14.548
30	Present ($\varepsilon_z \neq 0$)	5217.88	1.234	556.822	14.256	6741.24	1.564	686.92	22.017
	Kant et al. [44]	–	1.235	547.390	14.322	–	1.566	675.36	21.837
40	Present ($\varepsilon_z \neq 0$)	12,367.70	1.232	989.724	19.009	15,978.24	1.562	1221.01	29.375
	Kant et al. [44]	–	1.233	972.960	19.096	–	1.564	1200.48	29.124
50	Present ($\varepsilon_z \neq 0$)	24,155.11	1.231	1546.31	23.762	31,206.63	1.562	1907.69	36.729
	Kant et al. [44]	–	1.233	1520.00	23.870	–	1.564	1875.50	36.410

3.1 Numerical results

Numerical results for these problems are presented in Tables 3, 4, 5, 6, 7, 8, 9, 10, and 11, and graphically in Figs. 2, 3, 4, 5, 6, 7, 8, 9, 10, 11, and 12 followed by subsequent discussions. Interlaminar transverse shear and normal stresses cause delamination in multilayered composite structures. The evaluation of transverse shear stresses for the layered beam from the constitutive relations leads to discontinuity at the layer interface. Therefore, in the present study, these stresses are obtained by integrating the 2D elasticity equilibrium equations neglecting the body forces. These equations are as follows:

Table 4 Comparison of axial displacement, transverse displacement, axial stress, and transverse shear stress for two-layered (0°/90°) anti-symmetric laminated composite beam

L/h	Source	Sinusoidal loading				Uniform loading			
		$\bar{u}^{max}$	$\bar{w}^{max}$	$\bar{\sigma}_x^{max}$	$\bar{\tau}_{xz}^{max}$	$\bar{u}^{max}$	$\bar{w}^{max}$	$\bar{\sigma}_x^{max}$	$\bar{\tau}_{xz}^{max}$
4	Present ($\varepsilon_z \neq 0$)	1.718	4.396	33.825	2.989	2.268	5.523	40.494	5.078
	Reddy [11]	1.711	4.451	33.592	2.977	2.258	5.590	40.239	5.024
	Vidal and Polit [45]	–	4.682	30.800	2.761	–	–	–	–
	Maiti and Sinha [39]	–	3.534	25.783	2.846	–	–	–	–
	Kant et al. [44]	–	4.708	30.002	2.719	–	5.900	36.678	3.848
	Timoshenko [4]	1.421	4.797	27.905	2.947	1.836	6.009	34.427	4.557
	Bernoulli–Euler [2, 3]	1.421	2.625	27.905	2.947	1.836	3.330	34.427	4.557
10	Present ($\varepsilon_z \neq 0$)	22.935	2.911	180.543	7.385	29.799	3.683	221.402	11.586
	Reddy [11]	22.942	2.923	180.189	7.378	29.805	3.697	221.017	11.544
	Vo and Thai [27]	–	–	–	–	–	3.687	–	–
	Zenkour [37]	–	2.974	182.200	6.282	–	3.762	224.600	9.469
	Kant et al. [44]	–	2.961	176.530	7.255	–	3.744	217.33	10.738
	Timoshenko [4]	22.206	2.973	174.405	7.367	28.688	3.759	215.170	11.392
	Bernoulli–Euler [2, 3]	22.206	2.625	174.405	7.367	28.688	3.330	215.170	11.392

Table 5 Comparison of axial displacement, transverse displacement, axial stress, and transverse shear stress for three-layered (0°/90°/0°) symmetric laminated composite beam

L/h	Theory	Sinusoidal loading				Uniform loading			
		$\bar{u}^{max}$	$\bar{w}^{max}$	$\bar{\sigma}_x^{max}$	$\bar{\tau}_{xz}^{max}$	$\bar{u}^{max}$	$\bar{w}^{max}$	$\bar{\sigma}_x^{max}$	$\bar{\tau}_{xz}^{max}$
4	Present ($\varepsilon_z \neq 0$)	0.890	2.716	17.558	1.528	1.195	3.394	20.288	1.761
	Reddy [11]	0.865	2.700	16.990	1.557	1.162	3.368	19.671	1.831
	Chakrabarti et al. [46]	0.924	2.889	18.260	1.460	–	–	–	–
	Kant et al. [44]	–	2.890	18.819	1.577	–	3.605	21.584	2.488
	Timoshenko [4]	0.514	2.411	10.085	1.769	0.664	2.992	12.443	2.736
	Bernoulli–Euler [2, 3]	0.514	0.511	10.085	1.769	0.664	0.648	12.443	2.736
10	Present ($\varepsilon_z \neq 0$)	8.997	0.882	70.836	4.322	11.819	1.106	85.664	6.016
	Reddy [11]	8.940	0.875	70.213	4.334	11.734	1.098	85.030	6.090
	Vo and Thai [27]	–	–	–	–	–	1.108	85.66	4.533
	Chakrabarti et al. [46]	9.348	0.933	73.610	4.320	–	–	–	–
	Kant et al. [44]	–	0.933	73.660	4.239	–	1.171	89.120	6.150
	Zenkour [37]	–	0.873	70.210	–	–	1.096	85.060	4.289
	Timoshenko [4]	8.026	0.815	63.034	4.423	10.369	1.023	77.767	6.839
	Bernoulli–Euler [2, 3]	8.026	0.511	63.034	4.423	10.369	0.648	77.767	6.839

$$\tau_{xz}^{(k)} = -\sum_{k=1}^{N} \int_{z_k}^{z_{k+1}} \frac{\partial \sigma_x^{(k)}}{\partial x} \mathrm{d}z + C_1 \quad \text{and}$$
$$\sigma_z^{(k)} = -\sum_{k=1}^{N} \int_{z_k}^{z_{k+1}} \frac{\partial \tau_{xz}^{(k)}}{\partial x} \mathrm{d}z + C_2 \tag{33}$$

The interlaminar stresses of kth lamina can be evaluated by layerwise integration of Eq. (33) with respect to the thickness coordinate (z). The C_1 and C_2 can be determined by imposing the continuity and boundary conditions at the appropriate locations. Axial displacement (u), transverse displacement (w), bending stress (σ_x), transverse shear stress (τ_{xz}), transverse normal stress (σ_z), natural frequencies ($\bar{\omega}$), and critical buckling loads (N_{cr}) are presented in the following non-dimensional forms available in the literature.

$$\bar{u}\left(0, \frac{z}{h}\right) = \frac{E_3 u}{q_0 h},\ \bar{w}\left(\frac{L}{2}, \frac{z}{h}\right) = \frac{E_3 100 h^3 w}{q_0 L^4},\ \bar{\sigma}_x\left(\frac{L}{2}, \frac{z}{h}\right) = \frac{\sigma_x}{q_0},$$
$$\bar{\tau}_{xz}(0,0) = \frac{\tau_{xz}}{q_0},\ \bar{\sigma}_z\left(\frac{L}{2}, \frac{z}{h}\right) = \frac{\sigma_z}{q_0},\ \bar{\omega} = \frac{\omega L}{h}\sqrt{\left(\frac{\rho}{E_3}\right)_f}$$
$$\text{and } N_{cr} = \frac{N_0 a^2}{E_3 h^3} \tag{34}$$

Table 6 Comparison of axial displacement, transverse displacement, axial stress, and transverse shear stress for three-layered (0°/core/0°) symmetric sandwich beam

L/h	Source	Sinusoidal loading				Uniform loading			
		$\bar{u}^{max}$	$\bar{w}^{max}$	$\bar{\sigma}_x^{max}$	$\bar{\tau}_{xz}^{max}$	$\bar{u}^{max}$	$\bar{w}^{max}$	$\bar{\sigma}_x^{max}$	$\bar{\tau}_{xz}^{max}$
4	Present ($\varepsilon_z \neq 0$)	1.752	10.107	34.668	1.370	2.391	12.463	39.569	2.797
	Reddy [11]	1.739	10.034	34.181	1.372	2.365	12.455	39.161	2.662
	Kant et al. [44]	–	11.060	37.552	1.356	–	13.750	43.488	2.280
	Timoshenko [4]	1.012	5.2798	19.898	1.410	1.308	6.548	24.549	2.181
	Bernoulli–Euler [2, 3]	1.012	1.007	19.898	1.410	1.308	1.277	24.549	2.181
10	Present ($\varepsilon_z \neq 0$)	17.709	2.483	139.49	3.507	23.307	3.100	168.76	5.265
	Reddy [11]	17.670	2.477	138.90	3.509	23.240	3.092	168.13	5.287
	Kant et al. [44]	–	2.668	143.14	3.504	–	3.330	172.60	5.240
	Timoshenko [4]	15.821	1.691	124.36	3.526	20.439	2.121	153.43	5.452
	Bernoulli–Euler [2, 3]	15.821	1.007	124.36	3.526	20.439	1.277	153.43	5.452
20	Present ($\varepsilon_z \neq 0$)	130.471	1.378	513.23	7.037	169.480	1.735	629.97	10.779
	Reddy [11]	130.277	1.375	512.04	7.044	169.210	1.732	628.55	10.784
	Kant et al. [44]	–	1.425	516.40	7.040	–	1.793	633.20	10.660
	Timoshenko [4]	126.568	1.178	497.46	7.052	163.515	1.488	613.74	10.905
	Bernoulli–Euler [2, 3]	126.568	1.007	497.46	7.052	163.515	1.277	613.74	10.905
30	Present ($\varepsilon_z \neq 0$)	433.322	1.173	1136.10	10.562	561.224	1.482	1398.47	16.259
	Reddy [11]	432.734	1.171	1133.88	10.573	560.445	1.479	1395.79	16.270
	Kant et al. [44]	–	1.193	1137.62	10.560	–	1.507	1400.40	16.050
	Timoshenko [4]	427.168	1.083	1119.29	10.579	551.86	1.371	1380.92	16.358
	Bernoulli–Euler [2, 3]	427.168	1.007	1119.29	10.579	551.86	1.277	1380.92	16.358
40	Present ($\varepsilon_z \neq 0$)	1021.31	1.101	2008.12	14.086	1321.33	1.393	2474.33	21.725
	Reddy [11]	1019.97	1.099	2004.45	14.101	1319.58	1.391	2469.87	21.743
	Kant et al. [44]	–	1.112	2008.64	14.080	–	1.407	2475.04	21.440
	Timoshenko [4]	1012.54	1.049	1989.86	14.105	1308.12	1.330	2454.96	21.811
	Bernoulli–Euler [2, 3]	1012.54	1.007	1989.86	14.105	1308.12	1.277	2454.96	21.811
50	Present ($\varepsilon_z \neq 0$)	1989.48	1.067	3129.27	17.609	2572.61	1.352	3857.55	27.184
	Reddy [11]	1986.91	1.066	3123.75	17.628	2569.26	1.350	3850.80	27.209
	Kant et al. [44]	–	1.075	3127.50	17.060	–	1.361	3855.00	26.850
	Timoshenko [4]	1977.62	1.035	3109.15	17.632	2554.92	1.311	3835.87	27.264
	Bernoulli–Euler [2, 3]	1977.62	1.007	3109.15	17.632	2554.92	1.277	3835.87	27.264

where E_3 is the Young's modulus of middle layer. Material properties used in the above problems are shown in Table 2.

3.2 Discussion of results

3.2.1 *Problem* 1: Bending of isotropic beam

Table 3 shows comparison of non-dimensional displacements and stresses of thick isotropic beams subjected to sinusoidal and uniform loadings. The material properties are given in Table 2 (material 1). The numerical results are obtained for various aspect ratios (L/h) and compared with those of Reddy [11], Ghugal and Shimpi [13], Kant et al. [44], TBT [4], and CBT [2, 3]. The results of axial and transverse displacements are exactly matching with the results of exact plane stress elasticity solution given by Kant et al. [44] due to the inclusion of thickness stretching effect in the present theory whereas stresses are in good agreement with other higher-order theories for isotropic beam with aspect ratio 4 in which shear deformation is very significant. For moderately thick beams (L/h = 10–50), the results of displacements and stresses are in excellent agreement with those provided by Kant et al. [44] due to normal deformation effect.

Since the effect of thickness stretching is considered in the present theory, it provides the additional stiffness to the

Table 7 Comparison of non-dimensional vibration frequencies for laminated composite beams

Lamination scheme	E_1/E_2	Source	a/h				
			5	10	20	50	100
0°/90°	40	Present ($\varepsilon_z \neq 0$)	6.185	6.999	7.276	7.377	7.413
		Khdeir and Reddy [47]	6.128	6.945	–	–	–
		Aydogdu [48]	6.144	–	7.218	–	–
		Vo and Thai [49]	6.058	6.909	7.204	7.296	–
		Vo et al. [50]	6.090	6.918	7.207	–	–
		Matsunaga [51]	6.144	6.991	–	–	–
		Timoshenko [4]	5.953	6.882	–	–	–
		Bernoulli–Euler [2, 3]	7.124	7.269	–	–	–
0°/90°/0°	10	Present ($\varepsilon_z \neq 0$)	6.787	8.165	8.682	8.861	8.876
		Aydogdu [21]	6.760	8.161	8.684	8.852	8.876
		Khdeir and Reddy [47]	6.789	8.176	8.690	8.853	8.876
		Karama et al. [16]	6.795	8.176	8.690	8.853	8.876
	40	Present ($\varepsilon_z \neq 0$)	9.245	13.675	16.450	17.638	17.647
		Aydogdu [21]	9.168	13.552	16.308	17.455	17.641
		Reddy [11]	9.252	13.624	16.339	17.463	17.643
		Karama et al. [16]	9.208	13.614	16.337	17.462	17.643
		Khdeir and Reddy [47]	9.208	13.614	–	–	–
		Vo and Thai [49]	9.206	13.607	16.327	17.449	–
		Chalak et al. [52]	9.208	13.611	16.336	–	–
		Aydogdu [48]	9.207	–	16.337	–	–
		Vo et al. [50]	9.294	13.616	16.326	–	–
		Matsunaga [51]	9.817	14.149	–	–	–
		Timoshenko [4]	9.205	13.670	–	–	–
		Bernoulli–Euler [2, 3]	17.421	17.632	–	–	–

Table 8 Comparison of non-dimensional vibration frequencies for four-layered (0°/90°/90°/0°) laminated beams

L/h	Source	Modes of vibration			
		Mode-1	Mode-2	Mode-3	Mode-4
5	Present ($\varepsilon_z \neq 0$)	1.760	4.358	7.052	9.947
	Arya [53]	1.785	4.444	7.181	10.084
	Arya [53]	1.783	4.444	7.201	10.147
	Rao et al. [54]	1.814	4.530	7.234	9.931
10	Present ($\varepsilon_z \neq 0$)	2.290	7.066	12.225	17.466
	Reddy [11]	2.314	6.989	12.070	17.203
	Zhen and Wanji [55]	2.314	6.985	12.045	17.113
	Matsunaga [51]	2.309	6.975	12.033	17.100
	Timoshenko [4]	2.315	6.977	11.980	16.924
15	Present ($\varepsilon_z \neq 0$)	2.513	8.531	15.871	23.635
	Arya [53]	2.505	8.569	16.063	23.962
	Arya [53]	2.505	8.562	16.048	23.941
	Rao et al. [54]	2.513	8.660	16.330	24.436

Table 9 Comparison of non-dimensional vibration frequencies for three-layered (0°/core/0°) sandwich beams

L/h	Source	Modes of vibration			
		Mode-1	Mode-2	Mode-3	Mode-4
5	Present ($\varepsilon_z \neq 0$)	8.14	17.98	27.40	36.98
	Chalak et al. [52]	7.83	17.29	26.92	33.40
	Vidal and Polit [45]	7.83	17.31	26.97	33.37
	Kapuria et al. [56]	7.82	17.27	26.90	–
10	Present ($\varepsilon_z \neq 0$)	12.76	33.24	53.54	73.37
	Chalak et al. [52]	12.26	31.33	50.28	69.18
	Vidal and Polit [45]	12.26	31.33	50.31	69.26
	Kapuria et al. [56]	12.23	31.29	50.21	68.09
20	Present ($\varepsilon_z \neq 0$)	16.04	52.12	94.41	168.79
	Chalak et al. [52]	15.41	49.04	87.06	163.43
	Vidal and Polit [45]	15.41	49.04	87.07	163.69
	Kapuria et al. [56]	15.38	48.94	86.90	163.12

beam, because of which, results predicted by the proposed theory are higher than those predicted by the Euler–Bernoulli theory for low L/h ratios (thick beams) and approaches to thin beam limits (Euler–Bernoulli theory) for high L/h ratios. Higher-order theories which do not include this effect yield a marginal difference in the bending results compared to those of present theory.

Table 10 Comparison of non-dimensional critical buckling loads for laminated composite beams

Lamination scheme	E_1/E_2	Source	a/h				
			5	10	20	50	100
(0°/90°/0°)	10	Present ($\varepsilon_z \neq 0$)	4.724	6.804	7.641	7.913	7.953
		Aydogdu [48]	4.682	6.788	7.657	7.943	7.985
		Khdeir and Reddy [57]	4.736	6.813	7.668	7.948	7.985
		Karama et al. [16]	4.736	6.814	7.668	7.948	7.985
		Vo and Thai [49]	4.709	6.778	7.620	7.896	–
	40	Present ($\varepsilon_z \neq 0$)	8.617	18.833	27.079	30.892	31.527
		Aydogdu [48]	8.540	18.662	26.986	30.882	31.536
		Khdeir and Reddy [57]	8.613	18.832	27.086	30.903	31.540
		Chakrabarti [58]	8.590	18.772	27.039	–	–
		Karama et al. [16]	8.699	18.865	27.092	30.904	31.536
		Vo and Thai [49]	8.609	18.814	27.050	30.859	–
(0°/90°/90°/0°)	10	Present ($\varepsilon_z \neq 0$)	4.481	6.323	7.047	7.280	7.314
		Reddy [11]	4.457	6.292	7.018	7.253	7.287
		Timoshenko [4]	4.768	6.444	7.065	7.260	7.289
		Bernoulli–Euler [2, 3]	7.299	7.299	7.299	7.299	7.299
	40	Present ($\varepsilon_z \neq 0$)	8.356	17.794	25.001	28.218	28.747
		Reddy [11]	8.315	17.742	24.954	28.177	28.707
		Timoshenko [4]	9.316	18.940	25.535	28.294	28.738
		Bernoulli–Euler [2, 3]	28.889	28.889	28.889	28.889	28.889

Table 11 Comparison of non-dimensional critical buckling loads for three-layered (0°/core/0°) sandwich beams

Source	a/h				
	5	10	20	50	100
Present ($\varepsilon_z \neq 0$)	1.476	4.081	7.355	9.491	9.902
Reddy [11]	1.484	4.089	7.365	9.503	9.914
Timoshenko [4]	2.707	5.992	8.600	9.793	9.992
Bernoulli–Euler [2, 3]	10.059	10.059	10.059	10.059	10.059

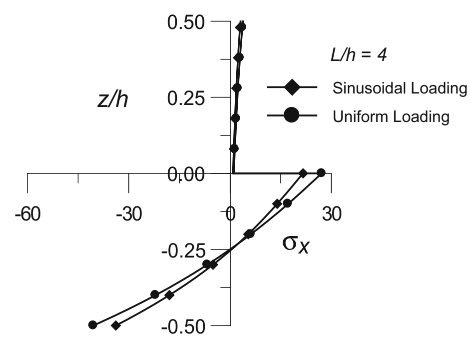

Fig. 3 Through-the-thickness variation of non-dimensional bending stress ($\bar{\sigma}_x$) at ($L/2$, z/h) in (0°/90°) beam under sinusoidal and uniform loadings

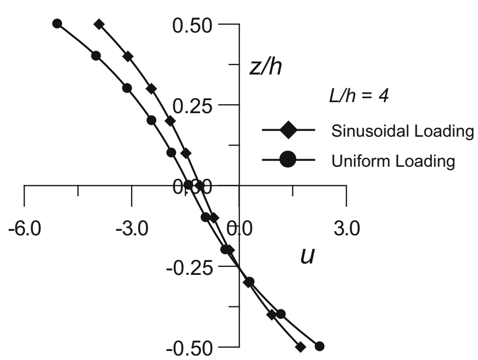

Fig. 2 Through-the-thickness variation of non-dimensional axial displacement ($\bar{u}$) at (0, z/h) in (0°/90°) beam under sinusoidal and uniform loadings

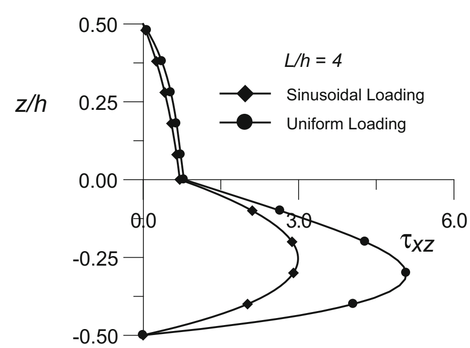

Fig. 4 Through-the-thickness variation of non-dimensional transverse shear stress ($\bar{\tau}_{xz}$) at (0, z/h) in (0°/90°) beam under sinusoidal and uniform loadings

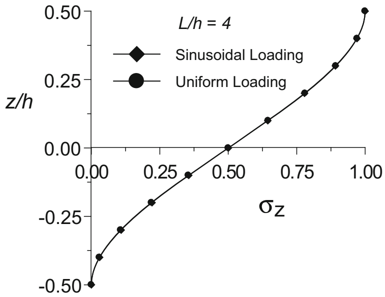

Fig. 5 Through-the-thickness variation of non-dimensional transverse normal stress ($\bar{\sigma}_z$) at ($L/2$, z/h) in (0°/90°) beam under sinusoidal and uniform loadings

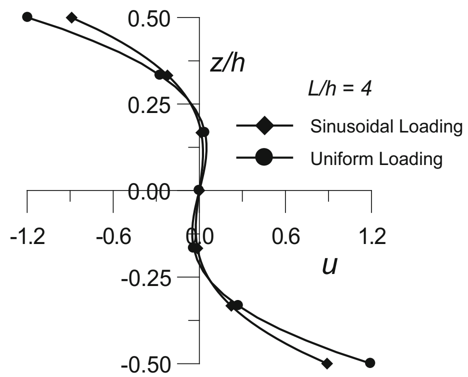

Fig. 6 Through-the-thickness variation of non-dimensional axial displacement ($\bar{u}$) at (0, z/h) in (0°/90°/0°) beam under sinusoidal and uniform loading

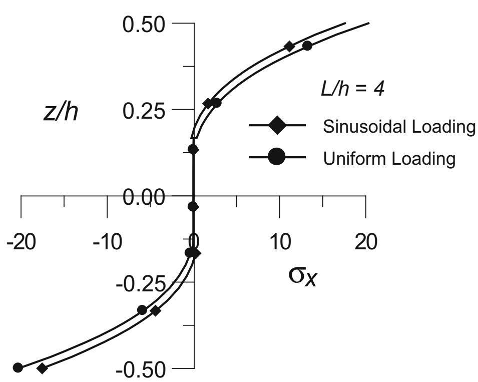

Fig. 7 Through-the-thickness variation of non-dimensional bending stress ($\bar{\sigma}_x$) at ($L/2$, z/h) in (0°/90°/0°) beam under sinusoidal and uniform loading

3.2.2 *Problem* 2: Bending of laminated composite beams

Tables 4 and 5 show the non-dimensional displacements and stresses of (0°/90°) and (0°/90°/0°) laminated beams, respectively. In both the lamination schemes, layers are of equal thickness and made up of material 2 (see Table 2). The displacements and stresses are obtained for aspect ratios 4 and 10. The present results are compared with

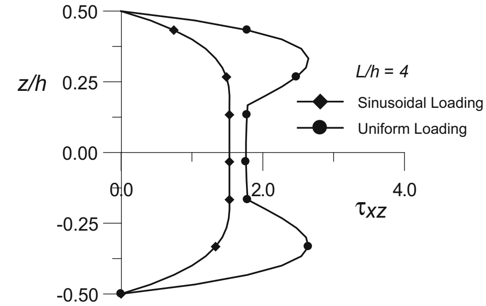

Fig. 8 Through-the-thickness variation of non-dimensional transverse shear stress ($\bar{\tau}_{xz}$) at (0, z/h) in (0°/90°/0°) beam under sinusoidal and uniform loadings

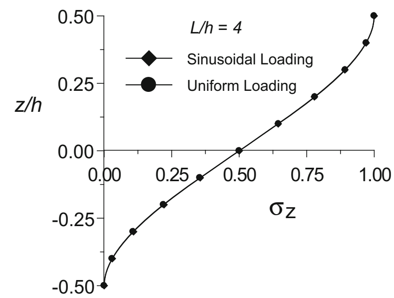

Fig. 9 Through-the-thickness variation of non-dimensional transverse normal stress ($\bar{\sigma}_z$) at ($L/2$, z/h) in (0°/90°/0°) beam under sinusoidal and uniform loadings

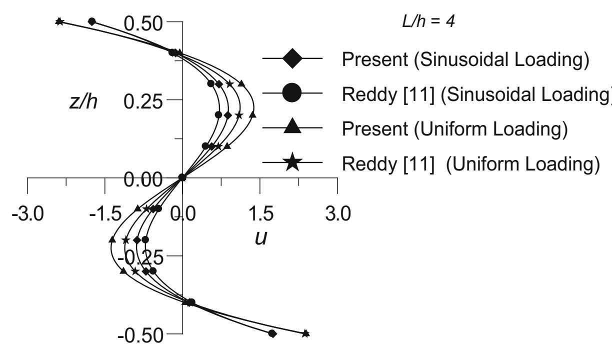

Fig. 10 Comparison of through-the-thickness variations of non-dimensional axial displacement ($\bar{u}$) at (0, z/h) in (0°/core/0°) beam under sinusoidal and uniform loadings

previously published results. The examination of Tables 4 and 5 reveals that the displacements and stresses in two-layered anti-symmetrically laminated beams are higher than those in three-layered symmetrically laminated beams. This is possibly due to presence of bending extension coupling stiffness which is zero in symmetrically laminated beams. Since the present theory considered the effect of transverse normal strain, i.e., thickness stretching, it provides the additional stiffness to the beam, because of which, results predicted by the present theory for (0°/90°/0°) laminated beams (see Table 5) are in excellent

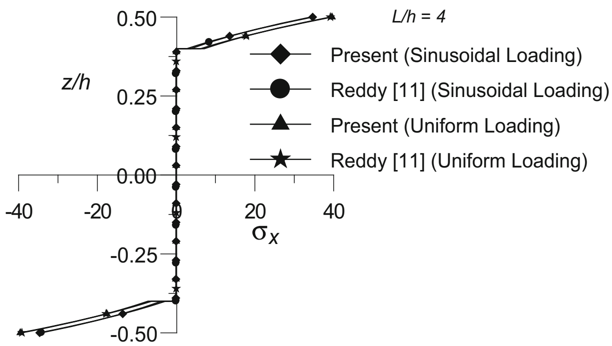

Fig. 11 Comparison of through-the-thickness variation of non-dimensional bending stress ($\bar{\sigma}_x$) at ($L/2$, z/h) in (0°/core/0°) beam under sinusoidal and uniform loadings

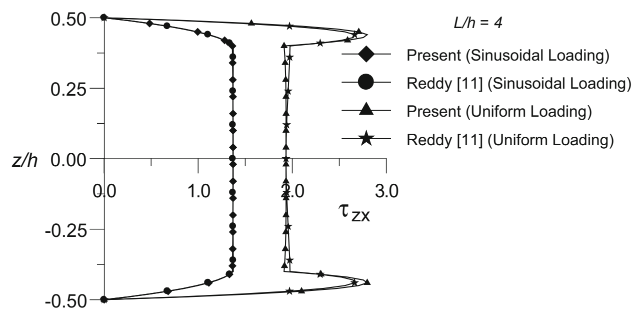

Fig. 12 Comparison of through-the-thickness variation of non-dimensional transverse shear stress ($\bar{\tau}_{xz}$) at (0, z/h) in (0°/core/0°) beam under sinusoidal and uniform loadings

agreement with those obtained by Chakrabarti et al. [46] using finite element analysis and plane stress solution given by Kant et al. [44]. Overall observations on Tables 4 and 5 show that the non-dimensional displacements and stresses obtained by using the present theory are in good agreement with those available in the literature. A large discrepancy in the displacements and stresses for laminated thick beam ($L/h = 4$) can be observed with the use of CBT [2, 3] and TBT [4] due to the neglect of transverse shear and normal deformations. However, for $L/h = 10$ results obtained using CBT [2, 3] and TBT [4] are in good agreement with each other. The through-the-thickness distribution of displacements and stresses for laminated composite beams under sinusoidal and uniform loading are shown in Figs. 2, 3, 4, 5, 6, 7, 8 and 9. Here, the through-the-thickness distributions of interlaminar transverse shear and normal stresses are obtained using equilibrium equations of theory of elasticity to ascertain stress continuity at layer interface. Figures 5 and 9 show that the value of transverse normal stress at the bottom surface of the beam is zero and equal to magnitude of transverse load at the top surface.

3.2.3 *Problem* 3: Bending of sandwich beams

Sandwich beam is a special form of laminated composite beam in which the modulus of core material is significantly lower than that of the face sheets. Therefore, study of global response of softcore sandwich structures is a challenging problem in numerical computation, especially using simplified (1D or 2D) theories, rather than 3D elasticity due to severe warping and normal deformation effects. Therefore, equivalent single-layer theories, which include effects of transverse normal strain, i.e., thickness stretching, are more effective for the analysis soft core sandwich beams. In this study, the present theory is applied for the bending of three-layered (0°/core/0°) symmetric sandwich beam. The beam has two face sheets (top and bottom) of thickness $0.1h$ each and thick soft core of thickness $0.8h$. The face sheets are made up of material 2 and core is made up of soft material 3. The material properties are given in Table 2. The comparison of non-dimensional displacements and stresses of the sandwich beam subjected to sinusoidal and uniform loading is given in Table 6. The exact elasticity solution for sandwich beam is not available in the literature. The examination of Table 6 reveals that the results of the present theory are in close agreement with those of plane stress elasticity solution given by Kant et al. [44]. This is the consequence of inclusion of the effect of thickness stretching in the present theory. The results of CBT deviate considerably, compared to those of refined theories due to the neglect of transverse shear and normal deformations. TBT showed similar trend for beams with low aspect ratios due to inclusion of only constant transverse shear strain in the theory. Comparison of through-the-thickness variations of non-dimensional axial displacement, bending stress, and transverse shear stress is shown in Figs. 10, 11, and 12. Considerable deviation in through-the-thickness variations of axial displacement is observed in Fig. 10, which shows that the present theory effectively captures the effect of soft core material compared to theory of Reddy [11] which neglect the effect of transverse normal deformation.

3.2.4 *Problem* 4: Free vibration of laminated composite beams

The effect of transverse normal deformation is equally important for the dynamic analysis of beams as in static bending of a beam. In this study, free vibration analyses of (0°/90°), (0°/90°/0°) and (0°/90°/90°/0°) laminated beams have been carried out using the present theory. In all the laminated beams, the overall thickness is equally distributed among all the layers. The material properties used are given in Table 2. The (0°/90°) and (0°/90°/0°) laminated beams are made up of material 4, whereas (0°/90°/

90°/0°) laminated beam is made up of material 5. The non-dimensional natural frequencies are shown in Tables 7 and 8. From the investigation of Tables 7 and 8, it is observed that the present results are in excellent agreement with those of refined theories available in the literature. Since the frequency of vibration is a global quantity with respect to the neutral axis of the beam, the effect of transverse normal deformation cannot be exhibited explicitly without exact solution, which is not available in literature.

3.2.5 *Problem* 5: Free vibration of sandwich beams

A three-layered (0°/core/0°) simply supported sandwich beam is analyzed in this problem using the present theory. The core has a thickness of $0.8h$, while it is $0.1h$ each for the two laminated face sheets. The face sheets are made up of material 6, whereas the core is made up of material 7 as given in Table 2. The values of the first four non-dimensional natural frequencies are presented in Table 9 for aspect ratios 5, 10, and 20. The present values of natural frequencies are in good agreement with those reported by Kapuria et al. [56], Chalak et al. [52], and Vidal and Polit [45]. Higher values of frequencies of present theory compared to other refined theories may be attributed to the thickness stretching effect which introduces an additional stiffness in transverse flexural vibration of beam. Since exact solution for this case is not available, the effect of thickness stretching on frequency response cannot be ascertained at present.

3.2.6 *Problem* 6: Buckling of laminated composite beams

This section presents the buckling behavior of laminated beam due to axial compressive forces. A symmetrically laminated beam is considered for the numerical study. Table 10 shows the comparison of the critical buckling load for (0°/90°/0°) and (0°/90°/90°/0°) laminated beams. The beam is analyzed by considering different modular ratios (E_1/E_2) and different aspect ratios (L/h). The beams are made up of material 4 as shown in Table 2. The results of present theory are compared with those published by Khdeir and Reddy [57], Aydogdu [48], Karama et al. [16] and Vo and Thai [49]. From the examination of Table 10, it is observed that the critical buckling loads for the four-layered symmetric beams are less than those of the three-layered beams. The increase in critical buckling load is observed with increase in aspect ratio as well as the modular ratio. The comparison of results with existing literature indicates that the results of the present theory are in very good agreement with those of other equivalent theories and may be due to inclusion of transverse normal strain effect.

The comparison of the critical buckling load for three-layered (0°/core/0°) sandwich plate is shown in Table 11. The composite face sheets are made up of material 2 and core is of material 3. The thickness of each face sheet is $0.1h$ and that of the core is $0.8h$. For the comparison purpose, results by using HSDT of Reddy [11], TBT of Timoshenko [4], and CBT of Bernoulli–Euler [2, 3] are specially generated. From Table 11, it is observed that the present results are in excellent agreement with those obtained by using HSDT of Reddy. The CBT results are independent of the aspect ratio (a/h), shear deformation being neglected in the theory.

In absence of an exact elasticity solutions for bending, buckling, and vibration of beams, the three-dimensional thick plate's origin of the sine shear function in one-dimensional analogue of thick plate, i.e., thick beam and the infinity of terms in its polynomial representation allow us to hope that the corresponding beam theory which includes thickness stretching effect will be accurate, without increasing the complexity compared to the TBT.

3.3 Recommendation for other boundary conditions of the beam

All the foregoing solutions are obtained for simply supported boundary conditions of the beam. For the other boundary conditions, the present theory can also be extended.

1. For the built-in boundary conditions, finite element method is widely used by various researchers. The present theory is simple and suitable for finite element formulation.
2. One can use general solution technique for the other boundary conditions of the beam by decoupling the governing equations from each other and solving them independently.
3. One can also use numerical methods such as discrete singular convolution method, Galerkin method, meshless method, radial basis functions, differential quadrature method, Rayleigh–Ritz method, and state-space method for the analysis of laminated composite beams with built-in boundary conditions.

4 Concluding remarks

Present paper deals with the assessment of trigonometric shear and normal deformation theory on bending, free vibration, and buckling analysis of isotropic, laminated composite, and sandwich beams. The present theory considers the effect of transverse shear deformation as well as the transverse normal strain, i.e., thickness stretching. The present theory satisfies the traction free boundary conditions at the top and bottom surfaces of the beam. The theory is variationally consistent and does not require shear correction factor. Navier-type closed-form solutions are obtained for bending, buckling, and vibration of simply supported beams and numerical results are presented. The numerical results for the displacements, stresses, natural frequencies, and critical buckling loads for standard problems of laminated composite and sandwich beams have shown the accuracy of the theory. Therefore, it is finally concluded that the effect of thickness stretching plays an important role while predicting bending, buckling and vibration responses of the laminated composite and sandwich beams. In the absence of an exact elasticity solution, numerical trend indicates that the results of present theory can be served as better reference solutions since the theory is represented by trigonometric functions which are correct from three-dimensional elasticity considerations.

References

1. Sayyad AS, Ghugal YM (2015) On the free vibration analysis of laminated composite and sandwich plates: a review of recent literature with some numerical results. Compos Struct 129:177–201
2. Bernoulli J (1694) Curvatura laminae elasticae. Acta Eruditorum Lipsiae 262–276 (Also in Bernoulli J (1744) Basileensis Opera 1(LVIII): 576)
3. Euler L (1744) Methodus inveniendi lineas curvas maximi minimive proprietate gaudentes. Apud Marcum-Michaelem Bousquet and Socio, Lausanne, Geneva, Switzerland, pp 1–322
4. Timoshenko SP (1921) On the correction for shear of the differential equation for transverse vibration of prismatic bars. Philos Mag 46:744–746
5. Timoshenko SP (1922) On the transverse vibrations of bars of uniform cross-section. Philos Mag 43:125–131
6. Carrera E (1999) A study of transverse normal stress effect on vibration of multilayered plates and shells. J Sound Vib 225(5):803–829
7. Carrera E (1999) Transverse normal stress effects in multilayered plates. ASME J Appl Mech 66(4):1004–1012
8. Carrera E (2005) Transverse normal strain effects on thermal stress analysis of homogeneous and layered plates. AIAA J 43(10):2232–2242
9. Levinson M (1981) A new rectangular beam theory. J Sound Vib 74:81–87
10. Krishna Murty AV (1984) Toward a consistent beam theory. AIAA J 22:811–816
11. Reddy JN (1984) A simple higher-order theory for laminated composite plates. ASME J Appl Mech 51:745–752
12. Kant T, Manjunatha BS (1989) Refined theories for composite and sandwich beams with C^0 finite elements. Comput Struct 33:755–764
13. Ghugal YM, Shimpi RP (2000) A trigonometric shear deformation theory for flexure and free vibration of isotropic thick beams. Structural Engineering Convention (SEC-2000), IIT Bombay, India
14. Sayyad AS, Ghugal YM (2015) Static flexure of soft core sandwich beams using trigonometric shear deformation theory. Mech Adv Compos Struct 2:45–53
15. Soldatos K, Elishakoff I (1992) A transverse shear and normal deformable orthotropic beam theory. J Sound Vib 155(3):528–533
16. Karama M, Afaq KS, Mistou S (2003) Mechanical behaviour of laminated composite beam by the new multi-layered laminated composite structures model with transverse shear stress continuity. Int J Solids Struct 40:1525–1546
17. Sayyad AS, Ghugal YM (2011) Flexure of thick beams using new hyperbolic shear deformation theory. Int J Mech 5(3):113–122
18. Sayyad AS (2012) Static flexure and free vibration analysis of thick isotropic beams using different higher order shear deformation theories. Int J of Appl Math Mech 8(14):71–87
19. Benatta MA, Mechab I, Tounsi A, Bedia EAA (2008) Static analysis of functionally graded short beams including warping and shear deformation effects. Comput Mater Sci 44:765–773
20. Benatta MA, Tounsi A, Mechab I (2009) Bouiadjra mathematical solution for bending of short hybrid composite beams with variable fibers spacing. Appl Math Comput 212:337–348
21. Aydogdu M (2009) A new shear deformation theory for laminated composite plates. Compos Struct 89:94–101
22. Mahi A, Bedia EAA, Tounsi A, Mechab I (2010) An analytical method for temperature-dependent free vibration analysis of functionally graded beams with general boundary conditions. Compos Struct 92:1877–1887
23. Shi G, Voyiadjis GZ (2011) A sixth-order theory of shear deformable beams with variational consistent boundary conditions. J Appl Mech 78:1–11
24. Sayyad AS, Ghugal YM, Naik NS (2015) Bending analysis of laminated composite and sandwich beams according to refined trigonometric beam theory. Curved Layer Struct 2:279–289
25. Sayyad AS, Ghugal YM (2016) On the free vibration of angle-ply laminated composite and soft core sandwich plates. J Sandw Struct Mater. https://doi.org/10.1177/1099636216639000 **(in press)**
26. Sayyad AS, Ghugal YM, Shinde PN (2015) Stress analysis of laminated composite and soft-core sandwich beams using a simple higher order shear deformation theory. J Serb Soc Comput Mech 9(1):15–35
27. Vo TP, Thai HT (2012) Static behavior of composite beams using various refined shear deformation theories. Compos Struct 94:2513–2522
28. Akavci SS (2010) Two new hyperbolic shear displacement models for orthotropic laminated composite plates. Mech Compos Mater 46:215–226
29. Ray MC (2003) Zeroth-order shear deformation theory for laminated composite plates. ASME J Appl Mech 70:374–380
30. Mantari JL, Oktem AS, Soares CG (2011) Static and dynamic analysis of laminated composite and sandwich plates and shells by using a new higher-order shear deformation theory. Compos Struct 94:37–49
31. Mantari JL, Oktem AS, Soares CG (2012) A new higher order shear deformation theory for sandwich and composite laminated plates. Compos B Eng 43:1489–1499
32. Mantari JL, Oktem AS, Soares CG (2012) A new trigonometric shear deformation theory for isotropic, laminated composite and sandwich plates. Int J Solids Struct 49:43–53
33. Meiche NE, Tounsi A, Ziane N, Mechab I, Bedia EAA (2011) New hyperbolic shear deformation theory for buckling and vibration of functionally graded sandwich plate. Int J Mech Sci 53:237–247
34. Daouadji TH, Henni AH, Tounsi A, Bedia EAA (2013) A new hyperbolic shear deformation theory for bending analysis of functionally graded plates. Model Simulat Eng 2012:1–10

35. Thai CH, Tran LV, Tran DT, Thoi TN, Xuan HN (2012) Analysis of laminated composite plates using higher-order shear deformation plate theory and node-based smoothed discrete shear gap method. Appl Math Model 36:5657–5677
36. Kant T, Manjunatha BS (1990) Higher-order theories for symmetric and un-symmetric fiber reinforced composite beams with C^0 finite elements. Finite Elem Anal Des 6:303–320
37. Zenkour AM (1999) Transverse shear and normal deformation theory for bending analysis of laminated and sandwich elastic beams. Mech Compos Mater Struct 6:267–283
38. Zenkour AM (1997) Maupertuis-Lagrange mixed variational formula for laminated composite structure with a refined higher order beam theory. Int J Non Linear Mech 32(5):989–1001
39. Maiti DK, Sinha PK (1994) Bending and free vibration analysis of shear deformable laminated composite beams by finite element method. Compos Struct 29:421–431
40. Sayyad AS, Ghugal YM (2011) Effect of transverse shear and transverse normal strain on bending analysis of cross-ply laminated beams. Int J of Appl Math Mech 7(12):85–118
41. Vo TP, Thai HT, Nguyen TK, Inam F, Lee J (2015) Static behaviour of functionally graded sandwich beams using a quasi-3D theory. Compos B Eng 68:59–74
42. Neves AMA, Ferreira AJM, Carrera E, Roque CMC, Cinefra M, Jorge RMN, Soares CMM (2011) Bending of FGM plates by a sinusoidal plate formulation and collocation with radial basis functions. Mech Res Commun 38:368–371
43. Neves AMA, Ferreira AJM, Carrera E, Roque CMC, Cinefra M, Jorge RMN, Soares CMM (2012) A quasi-3D hyperbolic shear deformation theory for the static and free vibration analysis of functionally graded plates. Compos Struct 94:1814–1825
44. Kant T, Pendhari SS, Desai YM (2007) On accurate stress analysis of composite and sandwich narrow beams. Int J Comput Methods Eng Sci Mech 8:165–177
45. Vidal P, Polit O (2010) Vibration of multilayered beams using sinus finite elements with transverse normal stress. Compos Struct 92:1524–1534
46. Chakrabarti A, Chalak HD, Iqbal MA, Sheikh AH (2011) A new FE model based on higher order zigzag theory for the analysis of laminated sandwich beam with soft core. Compos Struct 93:271–279
47. Khdeir AA, Reddy JN (1994) Free vibration of cross-ply laminated beams with arbitrary boundary conditions. Int J Eng Sci 32(12):1971–1980
48. Aydogdu M (2005) Vibration analysis of cross-ply laminated beams with general boundary conditions by Ritz method. Int J Mech Sci 47:1740–1755
49. Vo TP, Thai HT (2012) Vibration and buckling of composite beams using refined shear deformation theory. Int J Mech Sci 62:67–76
50. Vo TP, Thai HT, Inam F (2013) Axial- flexural coupled vibration and buckling of composite beams using sinusoidal shear deformation theory. Arch Appl Mech 83(4):605–622
51. Matsunaga H (2001) Vibration and buckling of multilayered composite beams according to higher order deformation theories. J Sound Vib 246(1):47–62
52. Chalak HD, Chakrabarti A, Iqbal MA, Sheikh AH (2011) Vibration of laminated sandwich beams having soft core. J Vib Control 18(10):1422–1435
53. Arya H (2003) A new zig-zag model for laminated composite beams: free vibration analysis. J Sound Vib 264:485–490
54. Rao MK, Desai YM, Chitnis MR (2001) Free vibration of laminated beams using mixed theory. Compos Struct 52:149–160
55. Zhen W, Wanji C (2008) An assessment of several displacement based theories for the vibration and stability analysis of laminated composite and sandwich beams. Compos Struct 84:337–349
56. Kapuria S, Dumir PC, Jain NK (2004) Assessment of zigzag theory for static loading, buckling, free and forced response of composite and sandwich beams. Compos Struct 64:317–327
57. Khdeir AA, Reddy JN (1997) Buckling of cross-ply laminated beams with arbitrary boundary conditions. Compos Struct 37(1):1–3
58. Chakrabarti A, Chalak HD, Iqbal MA, Sheikh AH (2011) Buckling analysis of laminated sandwich beam with soft core. Lat Am J Solids Struct 9:367–381
59. Cheng S (1979) Elasticity theory of plates and refined theory. ASME J Appl Mech 46:644–650